Weld World (2018) 62:117–130
DOI 10.1007/s40194-017-0517-y

RESEARCH PAPER

Effects of processing parameters on the characteristics of dissimilar friction-stir-welded joints between AA5058 aluminum alloy and PMMA polymer

Hamed Aghajani Derazkola[1] · **Reza Kashiry Fard**[2] · **Farzad Khodabakhshi**[3]

Received: 2 June 2017 / Accepted: 27 September 2017 / Published online: 11 October 2017
© International Institute of Welding 2017

Abstract In this research, newly modified solid-state friction-stir welding (FSW) technology was employed to bond the sheets of an aluminum-magnesium alloy (AA5058) and poly-methyl-methacrylate (PMMA) in a lap-joint design. Effects of processing parameters including tool rotational speed (w), traverse velocity (v), tilt angle and plunge depth on the surface morphology, materials flow pattern, microstructural characteristics, and mechanical properties of the dissimilar FSWed joints were studied. The geometry of U-antler macro-mechanical interlocking and interfacial micro- and nano-scale chemical bonding was mainly controlled by the tool tilting angle. A sound dissimilar weld with the highest tensile strength of around 45 MPa was attained at an optimum working window containing w = 1600 rpm, v = 25 mm/min, tool tilt angle of 2°, and plunge depth of 0.2 mm. Fracture of dissimilar lap joints occurred during transverse tensile-shear testing from the weld-polymer interface with a maximum strength ratio of ~ 60% by detachment of aluminum U-antler from the solidified polymer.

Recommended for publication by Commission XVI - Polymer Joining and Adhesive Technology

✉ Hamed Aghajani Derazkola
hamed.aghajani@srbiau.ac.ir

✉ Farzad Khodabakhshi
farzadkhodabakhshi83@gmail.com; fkhodaba@uwaterloo.ca

[1] Young Researchers and Elites Club, Science and Research Branch, Islamic Azad University, Tehran, Iran

[2] Department of Mechanical Engineering, Islamic Azad University, Kordestan Branch of Science and Research, Sanandaj, Iran

[3] School of Metallurgical and Materials Engineering, College of Engineering, University of Tehran, P.O. Box 11155-4563, Tehran, Iran

Keywords (IIW Thesaurus) Friction-stir welding · Dissimilar joint · AA5058 · PMMA · Tilt angle · Plunge depth

1 Introduction

In the last decade, dissimilar joining of polymers with the most of metals and alloys has attracted significant attentions to integrate the hybrid structures with a combined structural property for the aim of automotive industrial applications [1–3]. In this case, light metals such as aluminum and magnesium with the modern thermoplastics were of interest to reduce the fuel usage and CO_2 emission in the processed hybrid components, as the main factors [4]. Owing to large physical, chemical, and mechanical dissimilarities of the polymers and metals, several solid-state joining technologies were introduced for this aim [5, 6]. For instance, different joining technologies for fabrication of polymer-metal hybrid structures ranging from more conventional adhesive bonding and mechanical fastening to new welding-based technologies, such as ultrasonic welding [7] and induction welding [8] were categorized by Amancio et al. [5]. The mechanical property and failure behavior of the dissimilar polymer-metal joints prepared by injection clinching welding method as a technology based on staking and mechanical fastening were investigated by Abibe et al. [9]. Blaga et al. [10] examined the feasibility for dissimilar joining of glass-fiber-reinforced thermoplastic composites and titanium grade 2 using friction riveting technique. The feasibility and mechanical properties of ultrasonic spot-welded hybrid structures from an AA2024 aluminum alloy and a carbon-fiber-reinforced polymer were studied in the work of Balle et al. [11], as well. They showed a strength improvement up to two times higher with optimizing the processing parameters as compared to the weakest base alloy during quasi-static tensile shear loading [12]. In some other

works of those researchers [13–15], the effects of post heat treatment on the weldability of processed joints were investigated which the results showed significant improvements of shear strength. In a research by Bergmann and Stambke [16], laser welding was employed to join steel and polyamide. The effects of processing parameters and surface modifications on the weldability of these materials and subsequent mechanical performance were assessed, as well. Mitschang et al. [17] examined the feasibility of induction welding between steel and Al-Mg alloy with carbon-fiber-reinforced thermoplastic as well as the influence of different metal surface pretreatments on the shear strengths of processed dissimilar joints. However, modification and implementation of new born welding technologies are still required considering the large complexity of equipment and methods proposed so far with high production costs [18].

Recently, friction-stir welding (FSW) was developed as a new solid-state technology and employed for dissimilar joining of metals and polymers to make hybrid structures [3, 14, 18–22]. In this process, by plunging of a non-consumable rotating tool containing a shoulder and a pin into the edges of sheets with butt- or lap-joint designs, frictional and deformation heating is generated [23, 24]. Then, by tool traveling along the bond line and severe mixing of surrounded material as a result of material extrusion from leading to trailing edge, the weld nugget (WN) or stirred zone (SZ) is produced [25, 26]. As compared to the common fusion welding, mechanical fastening, or adhesive bonding processes, this new solid-state joining process is rapidly matured as a promising method due to the higher assembly rates and subsequent lower cost as well as the less material waste and avoid from radiation or harmful gas emission [25]. As the first attempt, the feasibility for dissimilar joining of AZ31 magnesium and glass fiber-reinforced polymer composite sheets was studied by using friction spot joining process in the work of Amancio-Filho et al. [3] which presented the possible physico-chemical and metallurgical transformations at the polymer and metal sides, respectively. Thereafter, Yusof et al. [27] assessed the friction stir spot lap joining of an aluminum-magnesium alloy with polyethylene (PET) and showed that the plunge speed as the main joining parameter possesses an impact influence on the heat generation to produce a sound dissimilar joint. Also, the friction spot welding of AA2024 aluminum alloy and phenylene sulfide in a single-lap joint design was evaluated by Goushegir et al. [28] and as a result, a correlation between the joining area and lap shear strength depended on the tool rotational speed was proposed. In the first work by F. Khodabakhshi et al. [18], they have optimized the processing parameters as the tool offset of 1.4 mm toward the aluminum side, tool rotational speed of 710 rpm, and traverse linear velocity of 63 mm/min to fabricate a sound dissimilar joint between the AA5059 aluminum-magnesium alloy and high-density polyethylene (HDPE) polymer. Also, they have studied the mechanical performance of processed dissimilar joints in the terms of joint strength and micro-hardness and showed some improvements of up to 50 and 200%, respectively, with failure location from the aluminum side. After that, in a new research [29], they have studied the possibility of macro-, micro-, and nano-scale bonding mechanisms between the aluminum and polymer by mixing during the FSW process as well as the nature of interface with using several normal and high-resolution electron microscopy analysis techniques. Consequently, they have proposed the interfacial physical/chemical interactions between aluminum and polymer with the formation of a thin semi-crystalline Al_2O_3 layer at the interface as the main bonding mechanism assisted by the mechanical interlocking and secondary Van der-Waals interaction. In the research of Liu et al. [30], restricting the air bubbles formation in the stirred region during FSW by controlling the processing parameters was found as the main effective method to enhance the strength of dissimilar joints between AZ31B magnesium alloy and MC nylon 6 with a lap-joint design. In some new researches by Ratanathavorn et al. [31] and Shahmiri et al. [21], the feasibility of dissimilar friction-stir welding of aluminum alloy to polypropylene sheets was studied. Also, the formation of dissimilar joints and subsequent mechanical properties depending on the main processing parameters of tool rotational speed and traverse velocity was assessed, as well. The reported maximum tensile-shear strength of the optimized processed dissimilar joints was about 20% of polypropylene as the weakest base material.

In following of previous researches, the main object of the present work was to investigate the effects of processing parameters on the microstructural and mechanical characteristics of dissimilar FSWs between the sheets of an AA5058 aluminum-magnesium alloy and poly-methyl-methacrylate (PMMA). The lap-joint design with placing the polymer material at top was considered into investigation. In previous studies, the effects of tool rotational speed (w) and traverse velocity (v) on the formation and property of dissimilar welds between aluminum and polymer were elaborated. Therefore, for the present research, those parameters were kept constant and the main focus would be on the other main processing parameters including tool plunge depth and tilting angle. A special design tool was used to increase the generation of aluminum fragments during melting of PMMA. Dissimilar joints formation and bonding mechanisms were studied by monitoring the materials flow pattern as well as the interface characterization using optical microscopy (OM) and scanning electron microscopy (SEM) equipped with energy-dispersive X-ray spectroscopy (EDS) analysis. Also, in the same procedure to previous publications [18, 21, 31, 32], the prepared dissimilar FSWed joints were evaluated in the terms of joint strength, fracture behavior, and microscopic examination of the weld cross section to find the optimum working window with maximum improvement in the tensile-shear strength.

2 Experimental procedure

In this research, the AA5058 aluminum-magnesium alloy and poly-methyl-methacrylate (PMMA) polymer sheets were utilized as the initial base materials. These plates were cut in the dimensions of 200 mm length, 50 mm width, and 4 mm thickness by using water-jet machining. AA5058 alloy is a commonly used material for automobile panel applications in the sheet form and PMMA is a special plastic that exhibits well thermal and chemical stability which usually required for light weighting systems and external body parts. These base materials possess great potentials for application in the automobile body structures. The main physical and mechanical properties of these base materials are expressed and compared in Table 1.

The lap-joint design with placing PMMA sheet on top was examined during friction stir welding to process an Al-polymer bi-materials structure from these dissimilar base materials. A flexible clamping system made of high-carbon steel was designed to clamp the plates during processing in their proper positions. In FSW process, a non-consumable tool containing a shoulder and a specific pin as well, is plunged on the surfaces of sheets to be welded [19, 33]. Friction at the surface between the shoulder and base material surfaces plays the main role to heat the work pieces. After plasticizing the surrounded material by frictional heating, the softened metals are forged, mixed, and extruded from the advancing side toward the retreating by the rotational tool stirring action, and as result the dissimilar weld nugget is formed [27, 34, 35]. Thus, the dissimilar weld metal is formed under the mechanical mixing due to severe plastic deformation condition of this solid-state joining technology [24, 36]. As it is well known, various processing parameters including the tool geometry and design, tool rotational speed (w), traverse velocity (v), tilting angle, and shoulder plunge depth possess impact influences on the properties of produced dissimilar FSWs [23]. Single-pass friction stir welds were conducted using a milling machine in position control mode and with an FSW tool made of tungsten carbide. Among the processing parameters, at first, the tool rotational speed and traverse velocity were optimized as w = 1600 rpm and v = 25 mm/min based on our previous researches [18, 29]. A wide range of other FSW parameters including the various tool plunge depths (0.1 to 0.4 mm) and tool tilt angles (0 to 2°) were assessed to establish a suitable working window for production of a defect-free sound dissimilar joint with acceptable surface appearance. A conic geometry was used for the FSW tool. It has a 20-mm-diameter shoulder with a conical cavity and a conical probe measuring 4 to 6 mm in diameter (smallest and biggest ones) with 4.8 mm in length.

Surface appearance and soundness of the processed dissimilar joints were assessed by electronic macro-imaging. For accomplishment of macro- and microstructural investigations, the metallographic samples were prepared parallel and perpendicular to the FSW direction from the dissimilar joints to examine the bonding mechanism and formation at two different cross sections. Then, the standard metallographic procedure including grinding with using different grades of emery SiC papers and final mechanical polishing on diamond pasts was performed on the samples. Materials flow pattern in the stir zone (SZ) between these two dissimilar base materials and their intermixing were observed and studied under a light optical microscope (VERSAMET-3) incorporated with an image analyzing software (Clemex-Vision). Also, a scanning electron microscope (SEM, VEGA/TESCAN-XMU, Russia) equipped with an energy-dispersive X-ray spectrometer (EDS) and a transmission electron microscope (TEM, JEOL 2000FX, Japan) equipped with an X-ray analysis detector as well were utilized to analyze the interaction between aluminum and polymer during FSW process for finding the contributed bonding mechanisms. As follows, tensile flow and fracture behaviors of the prepared dissimilar joints were assessed with employing the universal transverse tensile testing method. Tensile coupons were machined with the gauge length of 32 mm according to the ASTM E8M standard. Tensile tests were conducted at room temperature according to the requirements of ASTM D1002-05 standard. The cross-head speed was kept constant and about 2 mm/min during testing. For each welding condition, tensile testing was repeated at least three times and average values reported. Furthermore, the fracture surfaces of tensile-failed samples were studied under SEM, as well.

Table 1 The main physical properties of AA5058 aluminum alloy and poly-methyl-methacrylate (PMMA) polymer

Base materials	AA5058	PMMA
Glassy transition temperature (°C)	–	106
Density (kg/m^3)	2685	1190
Thermal conductivity (W/m.K)	193	0.2
Ultimate tensile strength (MPa)	145	77
Elongation (%)	24	6
Shear strength (MPa)	103	140

3 Results and discussion

3.1 Surface material flow

Figure 1 shows the welded dissimilar joints at processing conditions of w = 1600 rpm, v = 25 mm/min, tilt angle of 2°, and plunge depth of 0.2 mm. Color changing of PMMA from white toward the gray one can be noted, mainly due to fragmentation of aluminum lower part and introducing of aluminum particles within the polymer matrix. High-magnification SEM image from the surface of processed dissimilar joint is

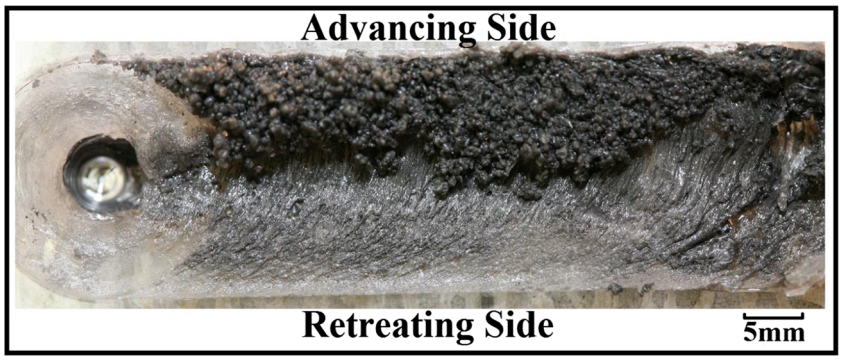

Fig. 1 Surface material flow appearance of the dissimilar welded joint at a processing parameter of w = 1600 rpm and v = 25 mm/min with controlling the tool tilt angle and plunge depth around 2° and 0.2 mm, respectively

presented in Fig. 2 and showing the presence of small aluminum particles with the white color contrast. Due to direct contact between the shoulder and surface of PMMA sheet, the size and density of aluminum particles are continuously decreased from the joint interface toward the polymer surface. Therefore, the structure of the upper part polymer at the stirred region can be considered as a composite with a functionally graded structure.

Figure 3a, b shows the surface appearances of the dissimilar FSWed joints with two different plunge depths of 0.1 and 0.2 mm, respectively. As seen and expected, with increasing plunge depth, the SZ color becomes more gray attributing to the presence of higher aluminum particles which indicate the better intermixing between aluminum and polymer during process. Tool plunge depth displays a direct impact influence on frictional heating between the rotating tool and base materials by increasing the axial force and hydrostatic pressure [23, 37]. In addition to a tunneling-like defect in the middle of dissimilar weld processed at lower plunge depth of 0.1 mm, many flashes and flakes due to excessive volatile material have deteriorated the dissimilar joint formation at higher plunge depth level of 0.4 mm. Therefore, the moderate value of 0.2 mm can be considered as the optimum plunge depth.

Effects of tool tilting angle in the range of 0° to 2° while the other parameters kept constant on the surface quality of processed dissimilar welds are demonstrated in Fig. 4. At lower tilt angles, the shape of dissimilar weld seems discontinuous due to interrupted material flow from forwarding to backing edge. Instability of tool movement during process can be found from the formation of a gray discrete layer on the surface. Meanwhile, with increasing tool tilt angle, surface appearance of dissimilar welds becomes more sound and homogenous. It can be attributed to more process stability by forging force increscent which provided more adequate conditions for material flow and extrusion from advancing side toward the retreating one. Also, increasing the titling angle can affect the aluminum and polymer interaction at the interface, as well

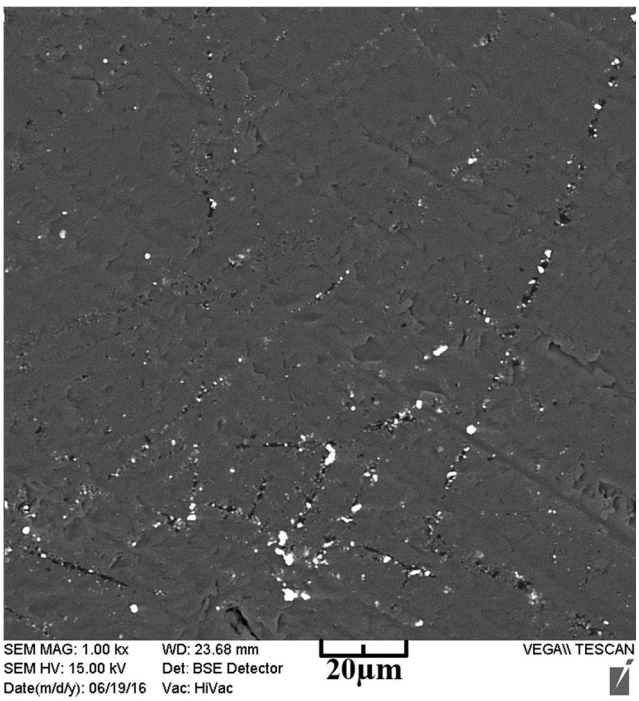

Fig. 2 SEM image from the distribution of aluminum particles within the PMMA matrix at the joint interface

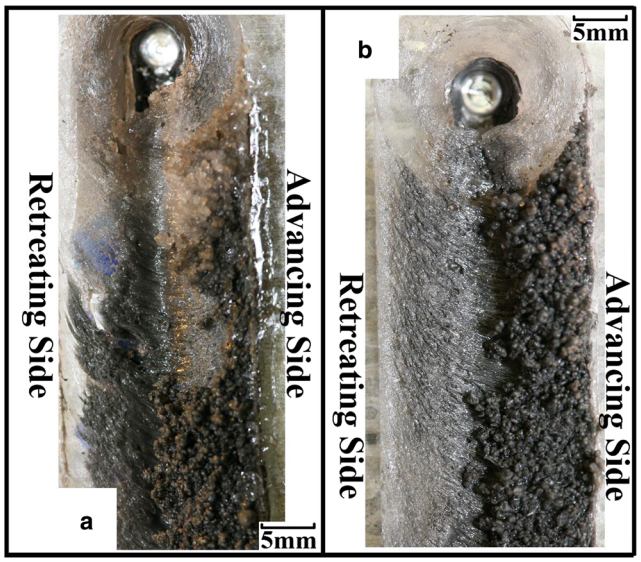

Fig. 3 Surface materials flow patterns of the prepared dissimilar joints at the same conditions with different plunge depths of 0.1 mm (**a**) and 0.2 mm (**b**)

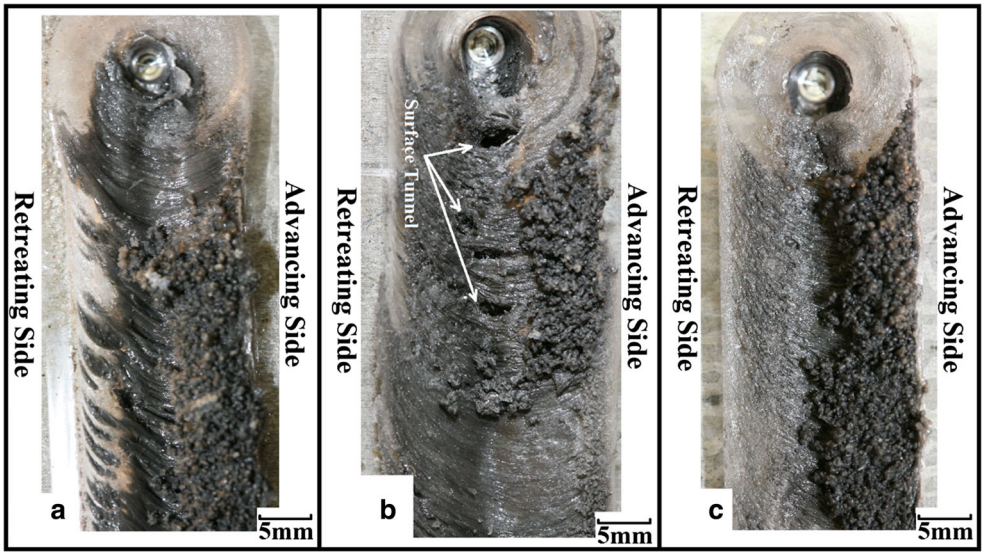

Fig. 4 Surface flow appearances of the processed dissimilar joints at the different tool tilt angles of 0° (**a**), 1° (**b**), and 2° (**c**)

and incorporate higher amounts of aluminum fragments from the aluminum-based alloy into the dissimilar weld zone. An indication for this matter is more color changing toward gray with continuous increasing of tool tilting angle. Therefore, the best condition is attained at the higher title angles.

3.2 Macrostructure of dissimilar joints

A schematic representation from the dissimilar mixing of the examined base materials across the thickness section during FSW process is shown in Fig. 5. As it is well known and also indicated in this plot as well, during friction stirring process, material at advancing side expect higher frictional heating and severe plastic deformations. Therefore, the size of heat (HAZ) and thermo-mechanical-affected zones (TMAZ) in both dissimilar materials would be larger at advancing side as compared to the retreating one. Also, changing the processing parameters can affect this cross-sectional macro-profile and subsequent metallurgical aspects, as well [23, 37, 38]. The cross-sectional views of macrostructures for the processed dissimilar welds at different tilt angles and plunge depths are presented in Figs. 6 and 7, respectively. For all conditions, the dissimilar SZ can be clearly distinguished by fine aluminum fragments within the melted and re-solidified PMMA matrix with black color contrast. Also, a U-antler with two aluminum ramus was formed at the center of SZ for all joints. These ramus were formed along the joint line for both advancing and retreating sides. They were produced because of less heat generation to completely plasticize the aluminum as shoulder in direct contact with the PMMA surface. Furthermore, low heat transfer coefficient of PMMA can restrict the heat flux toward AA5058 aluminum alloy, as well. However, the

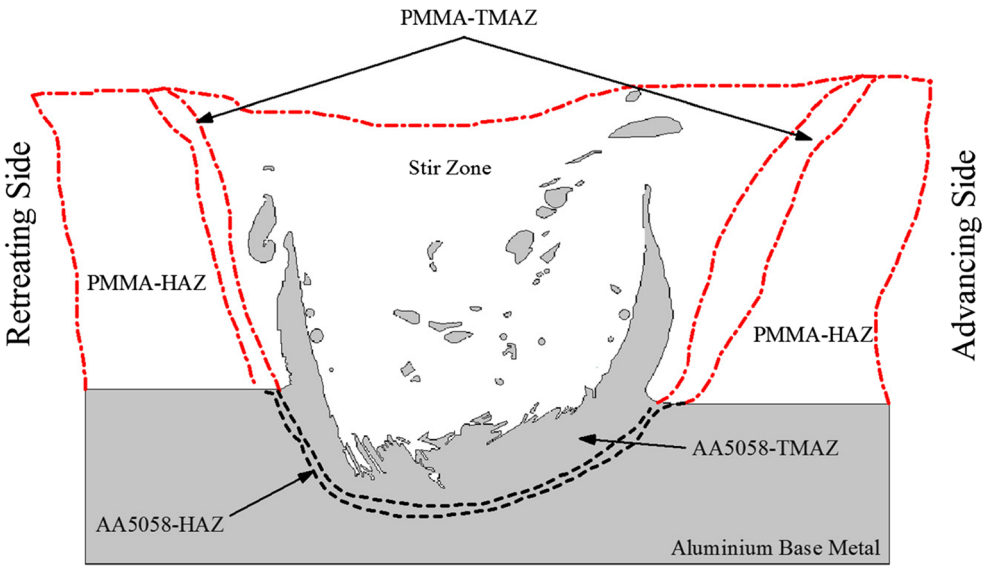

Fig. 5 Schematic representation of dissimilar FSW formation between Al and polymer within the SZ

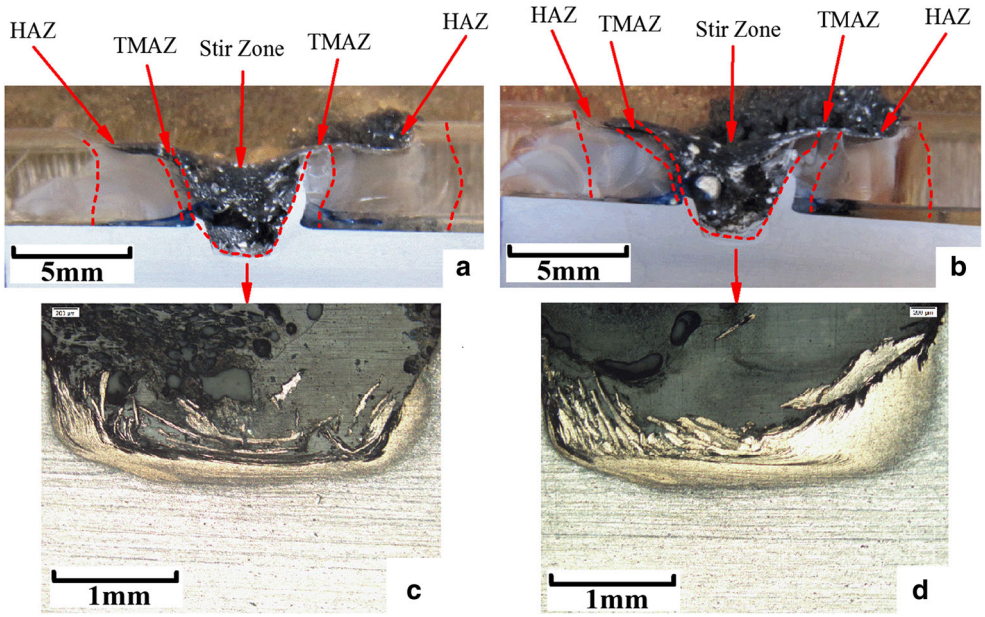

Fig. 6 Cross-sectional macrostructures for the PMMA and aluminum sides of welded joints with tool tilt angles of 0° (**a**, **c**) and 1° (**b**, **d**)

formation of these antennas during dissimilar bonding process can improve the macro- and micro-mechanical interlocking mechanisms, significantly and as a result, increase the joint strength. As shown in Figs. 6 and 7, the shape of this U-antler for macro-locking and other micro-locking features can affect the processing parameters, considerably. Thicker arm of advancing side as compared to the retreating one for all processed dissimilar welds is a noticeable issue which can be due to larger deformations at this region [27]. In simple comparison between the optical macro- and micro-graphs of Figs. 6 and 7, formation of higher volume fractions of air bubbles at lower tilt angles and plunge depths can be noticed. Higher tilt angle provides suitable condition for bubbles floating outside of the melted nugget. Although, increasing the forging pressure can exhibit the same effect as well by imposing an external hydrostatic pressure. As shown in the optical microscopy images, a TMAZ region surrounded by a thin dark HAZ region was formed in the lower part of AA5058 aluminum alloy. Also, with decreasing tilt angle and plunge depth, the HAZ area becomes narrower caused by the low-temperature thermo-mechanical interaction between the rotating tool and surrounding material. However, increasing the tool tilting angle and forging can cause the formation of bigger SZs between the dissimilar PMMA polymer and AA5058 aluminum alloy as well as the broader HAZ and TMAZ areas. As an interesting effect, the aluminum ramus bended outside of SZ at higher forging pressures (see Fig. 7b, d). It can be due to agglomeration of melted PMMA and imposing a high lateral pressure

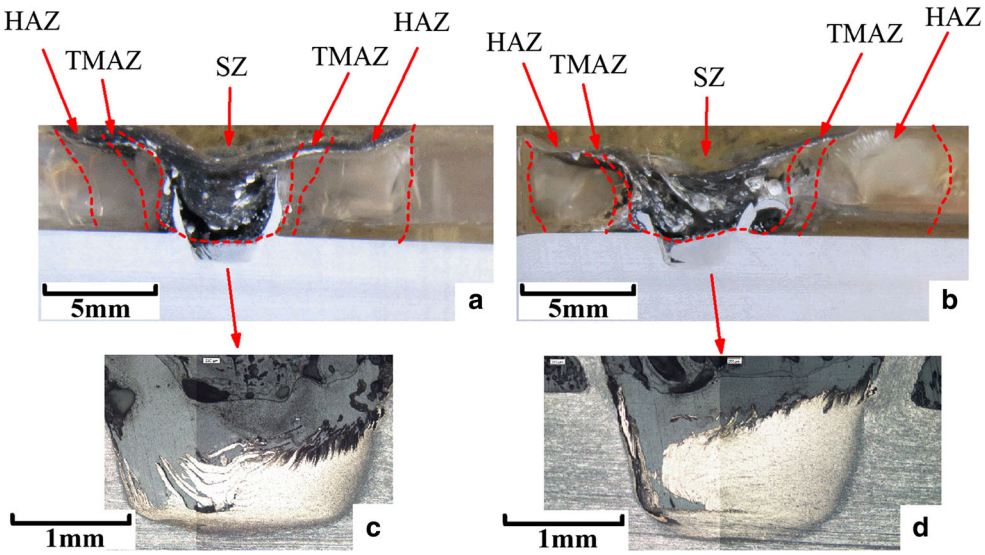

Fig. 7 Cross-sectional macrostructures for the PMMA and aluminum sides of welded joints with tool tilt angle of 2° and different plunge depths of 0.2 mm (**a**, **c**) and 0.4 mm (**b**, **d**)

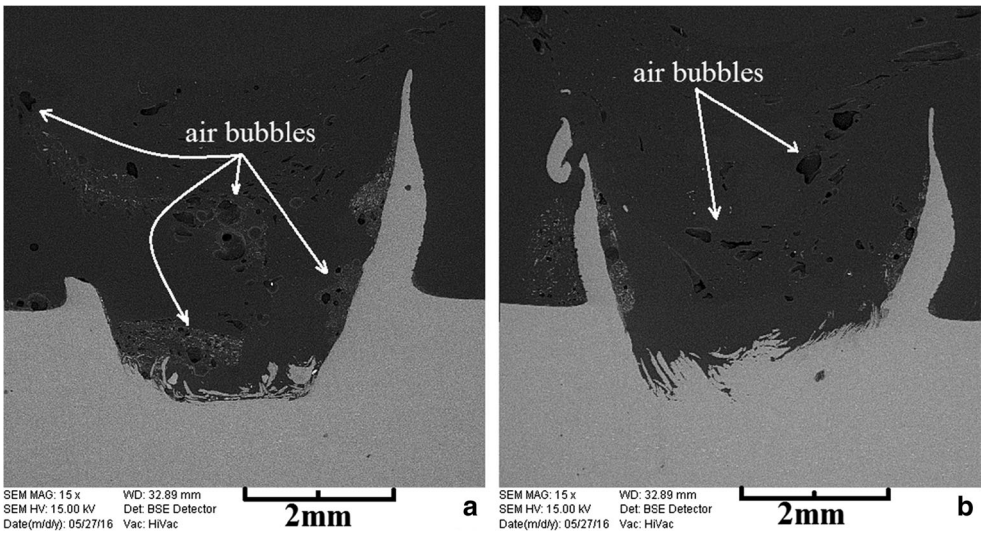

Fig. 8 SEM images showing the formation of macro-mechanical interlocks and soundness of the prepared dissimilar joints at the tool tilt angles of 0° (**a**) and 2° (**b**) with controlling a constant plunging depth of 0.2 mm

into the solidified aluminum ramuses during the stirring action. Also, the TMAZ exhibit a wavy morphology in this sample which experienced a metamorphosis and formed discontinuously in retreating side. As can be found from the presented results, the formation of dissimilar weld nugget between PMMA and AA5058 aluminum alloy is very sensitive to the tool plunge depth. However, changing the tool tilting angle did not display significant influence on the dimension and geometry of dissimilar SZ.

3.3 Internal material flow pattern, intermixing, and interface characterization

Effects of tool tilting angle at a constant plunge depth on the cross-sectional material flow pattern and internal mixing for the processed dissimilar joints are presented in SEM images of Fig. 8. As seen, with increasing tilt angle up to 2°, a wavy dent interface is formed at the TMAZ and SZ regions of aluminum material, as compared to the formation of big aluminum

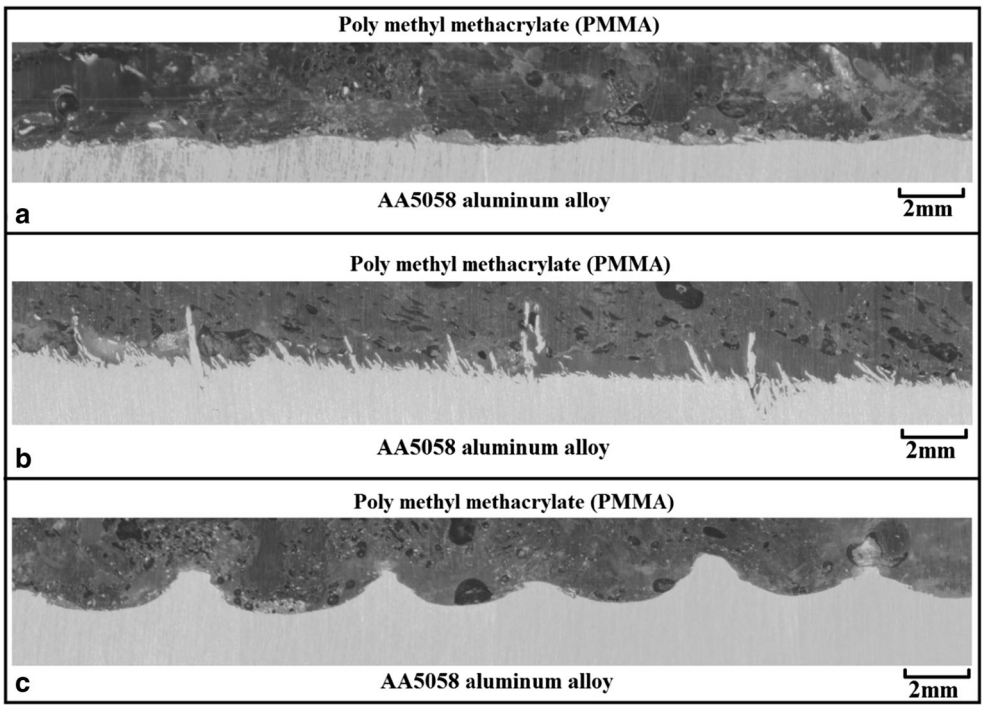

Fig. 9 Longitudinal cross-sectional flow patterns of the dissimilar welded joints at the tool tilt angles and plunge depths of 0°–0.1 mm (**a**), 2°–0.2 mm (**b**), and 2°–0.4 mm (**c**)

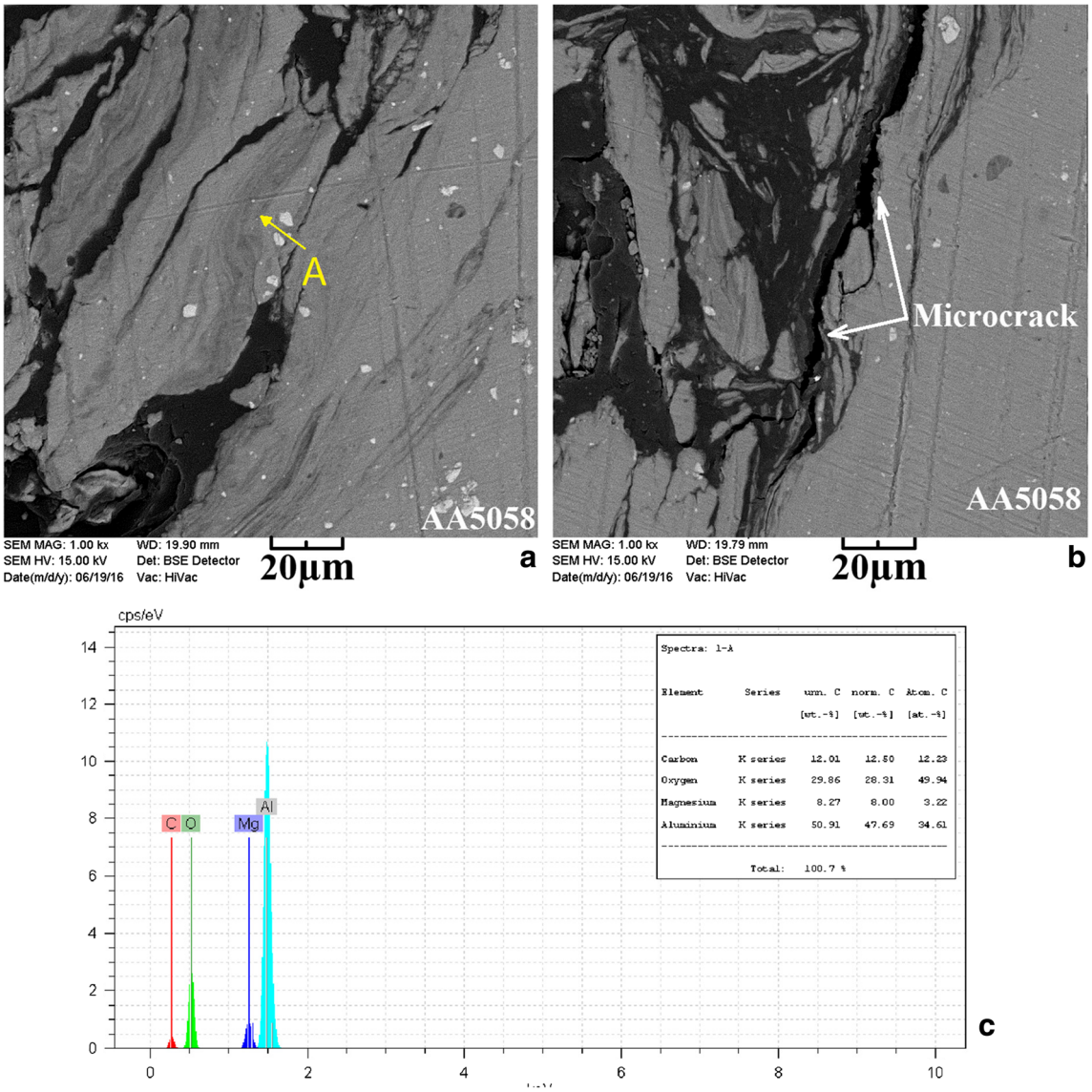

Fig. 10 High-magnification SEM images from the Al-polymer interfaces at the retreating (**a**) and advancing (**b**) sides of the dissimilar FSWed joint with plunge depth of 0.2 mm at tool tilt angle of 0°. **c** The EDS elemental analysis spectrum from the indicated point A in Fig. 9a

particles at lower tilt angles. Formation of mechanical interlocks between the aluminum of TMAZ and re-solidified PMMA of SZ depending on the tilting angle can be varied to the extent of common interfaces as controlled by the fragmentation of aluminum chips from the TMAZ into the SZ. However, in a simple comparison between Fig. 8a, b, it can be found that the size of aluminum fragments and interlocks is increased by increasing the tool tilt angle, due to higher surface tractions and severe wear phenomena during friction stirring. In these internal material flow studies, air bubbles formation due to shrinkage after melting and re-solidification of PMMA within the SZ during FSW process is also demonstrated in Fig. 8. As shown, more and bigger air bubbles are formed at lower title angles owing to unfortunate heat generation [9, 39].

Longitudinal micro-profiles from the thickness cross section of processed dissimilar welds at different tool tilting angles and plunge depths are presented in Fig. 9. Changing in the material flow pattern, intermixing/locking, and interface morphology by varying the processing parameters can easily be determined by comparing these longitudinal macrostructures. As shown, at low tilt angle and plunge depth, the joint interface seems smooth, some deal with limited numbers of mechanical interlocks, which indicate the weak bonding between the aluminum and polymer as caused by the low forging and extrusion forces during process (Fig. 9a). With concomitant increasing of tool tilt angle and plunge depth, the interface changes to a wavy shape due to vertical and horizontal material flow and intermixing by severe stirring action of the rotating tool [3, 5, 37, 39]. For instance, at tilt angle of 2° and

plunge depth of 0.2 mm, a semi-sharp interface with considerable numbers of mechanical interlocks is formed between the aluminum alloy and PMMA polymer (see Fig. 9b). At high plunge depth of 0.4 mm, a wavy morphology like the explosive welding process [40] can be observed between aluminum and polymer during mixing. As shown in Fig. 9c, large interface due to such corrugating-like morphology can make good chance for mechanical interlocking and chemical bonding, despite of big air bubbles with high concentrations due to turbulent flow. These morphological features at the interfaces can control the tensile-shear fracture behavior of these dissimilar joints as follows, as well.

Higher magnification SEM images and EDS chemical analysis results from advancing and retreating sides of processed dissimilar joints with different tool tilting angles of 0° and 2° at a constant plunge depth of 0.2 mm are presented in Figs. 10 and 11, respectively. Formation of a lamellar structure close to the advancing side with mixing of aluminum particles and PMMA polymer can be noticed. Due to less heat generation at the retreating side [23] and large difference between the coefficient of thermal expansion for PMMA and aluminum alloy [18], only some micro-locks can be formed during cooling process which leads to the less adhesion as compared to the advancing side. Furthermore, by comparison between the presented results in Figs. 10 and 11, it can be found that the physical/chemical interactions between these dissimilar base materials due to frictional heating and stirring action are intensified by increasing the tool tilting angle. Increase in the thickness of the lamellar structure at advancing side and low width of micro-locks at retreating side can be caused by these

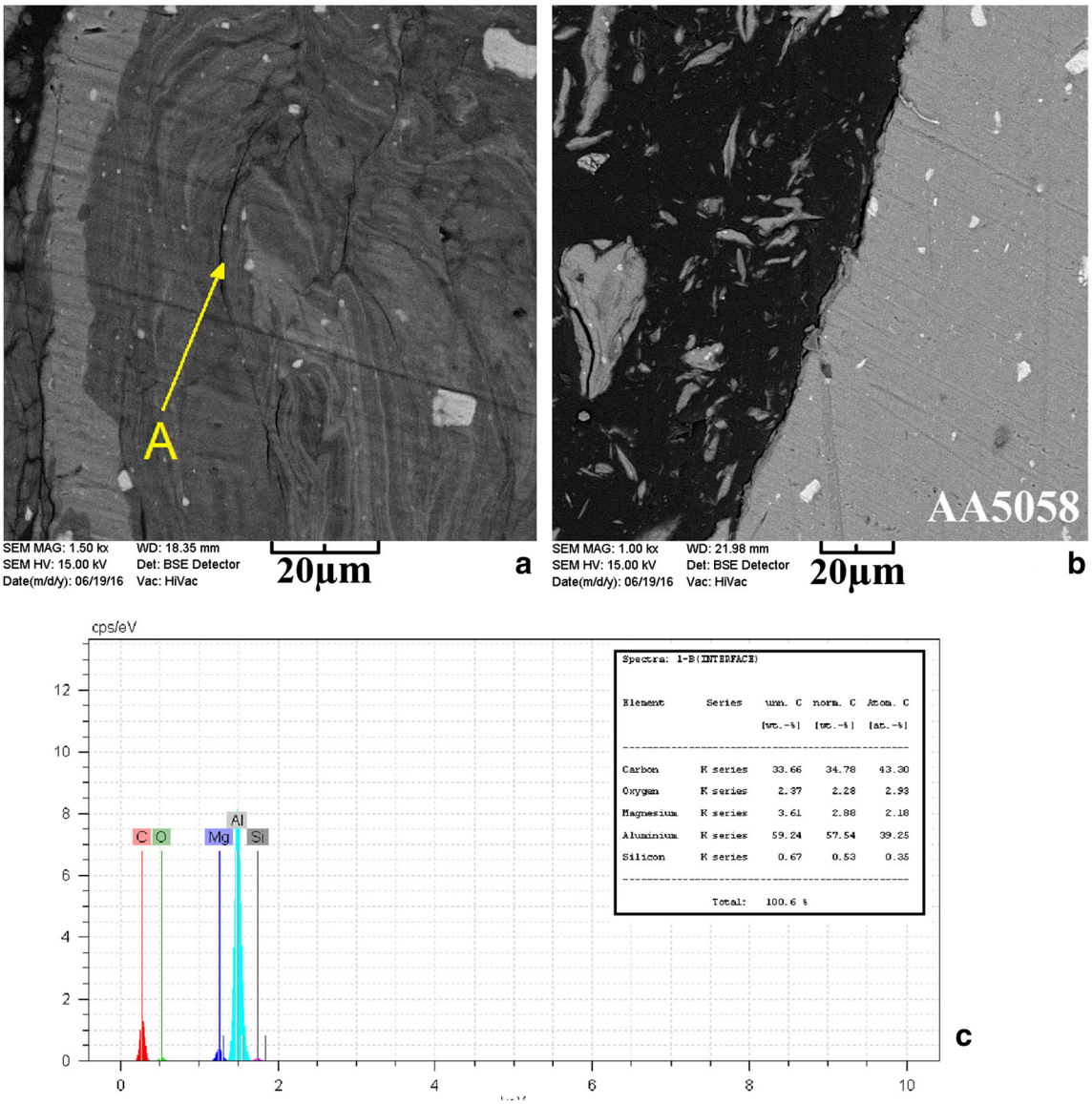

Fig. 11 High-magnification SEM images from the Al-polymer interfaces at the retreating (**a**) and advancing (**b**) sides of the dissimilar FSWed joint with plunge depth of 0.2 mm at tool tilt angle of 2°. **c** The EDS elemental analysis spectrum from the indicated point A in Fig. 10a

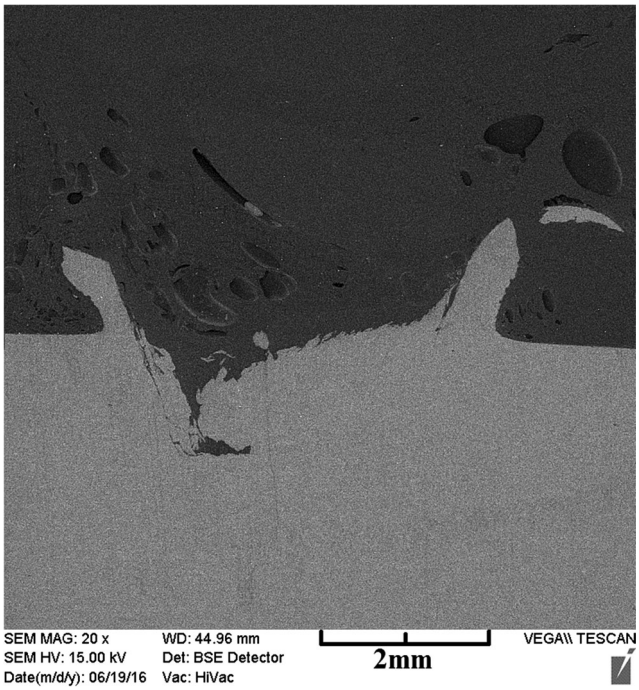

Fig. 12 Internal materials flow pattern and macro-mechanical interlocking for the processed dissimilar weld at the tool tilt angle of 2° and plunge depth of 0.4 mm

thermo-mechanical effects, as well. Chemical analysis results from the interfaces between aluminum and polymer at SZ indicate the presence of oxygen beside aluminum, magnesium, and carbon elements. Analysis of the interaction layer between aluminum alloy and re-solidified polymer requires TEM analysis to study the possible mechanisms with more details, as the results will be presented as follow.

Figure 12 shows the SEM image from cross section of processed dissimilar joint with plunge depth of 0.4 mm. High-magnification SEM images and EDS analysis results from the aluminum and polymer interfaces are presented in Fig. 13, as well. As seen, the plunge depth of higher than 0.2 mm possess a deteriorative influence on the formation of U-antler macro-lock and other micro-locks between the aluminum and polymer due to more heat generation at higher welding axial forces and pressures. It can lead to the formation of a broader TMAZ region, smaller aluminum particles, and bigger air bubbles, as well. As shown, some big aluminum fragments and thin gray veins are formed at both advancing and retreating sides of dissimilar weld. In the EDS analysis results, high amount of oxygen is detected as before, which indicates the formation of some continuous aluminum oxide veins due to

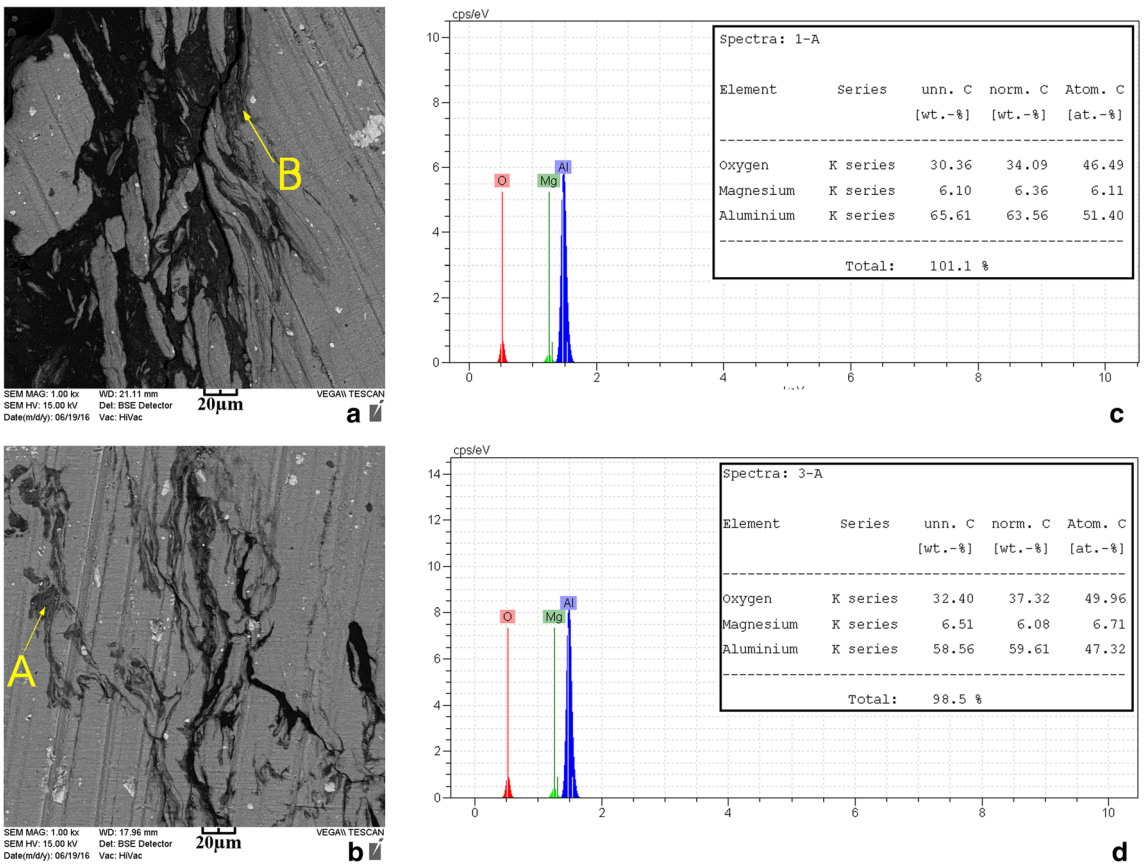

Fig. 13 SEM images (**a**, **c**) and EDS elemental analysis (**b**, **d**) results from two selected regions at the retreating (**a**, **b**) and advancing (**c**, **d**) sides of the welded joints at a tool tilt angle of 2° with a plunge depth of 0.4 mm

polymer thermal degradation during stirring of aluminum alloy. The oxide layer exhibits a continuous and cluster shape at the inner area of the aluminum U-antler as compared to the processed samples with lower plunge depths.

High-magnification TEM images combined with the elemental EDS mapping analysis results from a trapped aluminum particle within the polymer matrix are presented in Fig. 14. More accommodation of oxygen element on the surface of aluminum particle during process can indicate the formation of a thin alumina oxide layer as a result of liquid- and solid-state chemical reactions. This matter can add a secondary chemical bonding effect between aluminum and melted/re-solidified polymer during dissimilar FSW process beside of micro- and macro-locking mechanisms as discussed before. As proposed by Khodabakhshi et al. [18, 29], macro-, micro-, and nano-mechanical interlocking during low-temperature severe plastic deformation of FSW process assisted by the formation of a nano-sized semi-crystalline Al_2O_3 layer at the interfaces as well as the secondary Vander-Waal's interaction can be considered as the main dissimilar bonding mechanisms between aluminum fragments and polymer matrix at the SZ. The same features were observed in the present research, as well. Meanwhile, the fragmentation of aluminum chips from cutting edges by the screw action of the rotating tool and subsequent physical/chemical interactions can be affected by the tool tilting angle and plunge depth, as expressed before [25, 41]. The size of aluminum fragments increases at higher tilt angles and plunge depths due to changing in the thermo-mechanical behavior as well as the better vertical and horizontal circulations of molten thermoplastic which can leads to improving the adhesion effects by topographical interlocking phenomena. These effects can avoid void formation and non-uniform mixing as well, which possess detrimental influences on the dissimilar joints strength.

3.4 Tensile strength

Transverse tensile loading response of the processed dissimilar joints at various tool tilting angles and plunge depths during FSW process is demonstrated in Fig. 15a. The effects of tool tilt angle and plunge depth on the corresponding fracture behavior of these dissimilar FSWs are presented in macro-

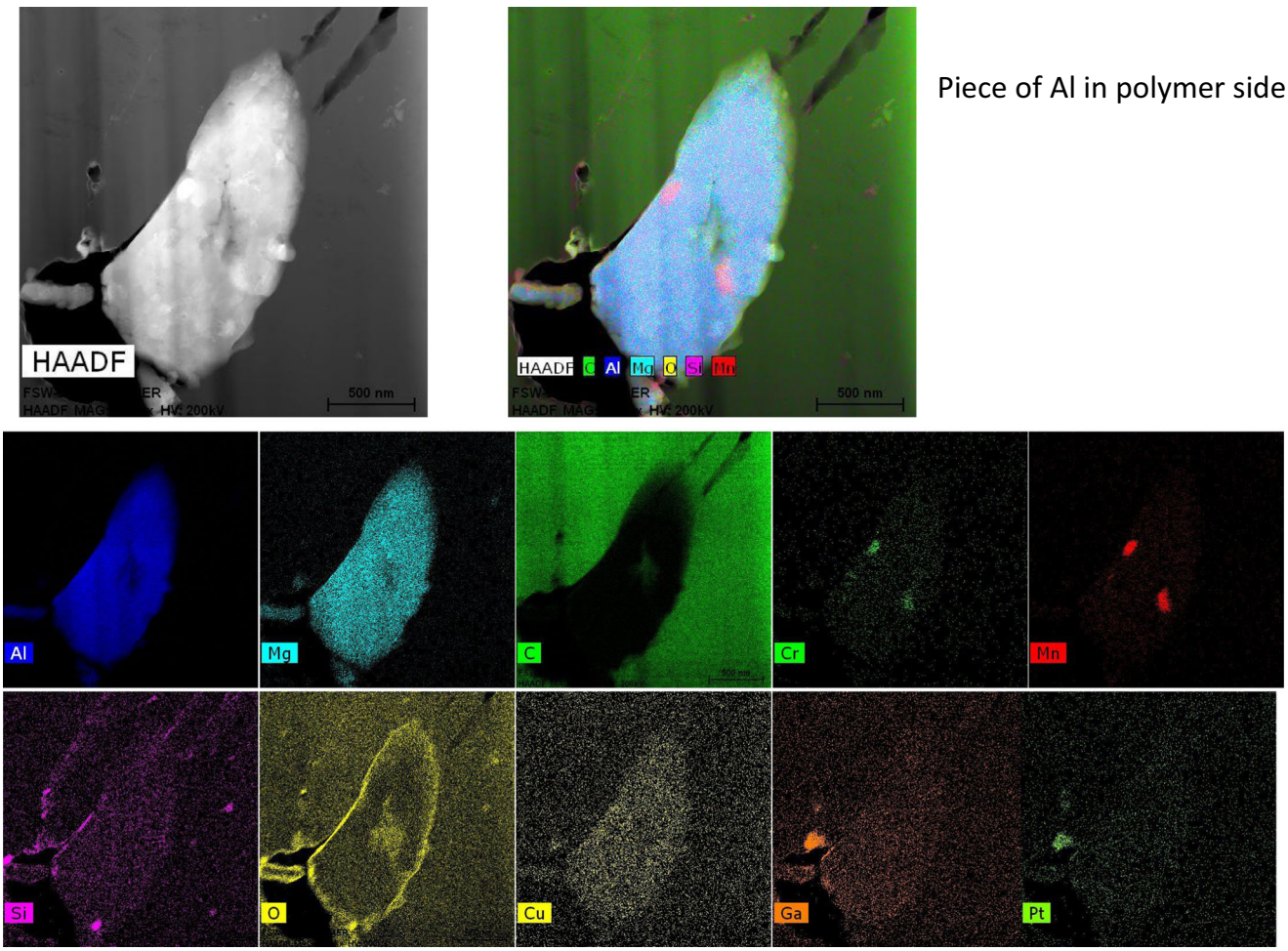

Fig. 14 High-magnification TEM imaging and elemental mapping results from a trapped aluminum particle within the polymer matrix

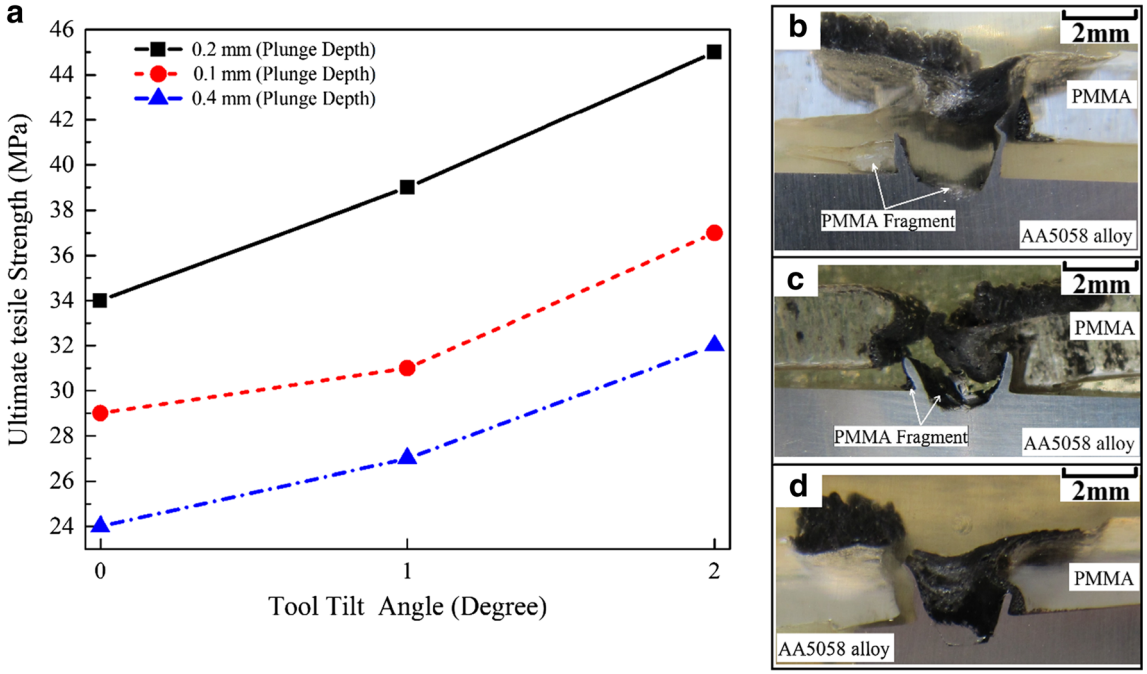

Fig. 15 **a** Effects of tool tilt angle and plunge depth on the ultimate tensile strength of the processed dissimilar joints. Fracture locations for the dissimilar FSWs prepared at the tool tilt angles and plunge depths of 0°–0.1 mm (**b**), 2°–0.1 mm (**c**), and 2°–0.4 mm (**d**)

images of Fig. 15b–d, respectively. As seen, with increasing tool tilting angle in the range of 0°–2° at a constant plunge depth, the ultimate tensile strength is increased, continuously. However, with increasing tool plunge depth in the range of 0.1–0.4 mm, tensile strength is increased at first up to 0.2 mm and thereafter reduced. As explained before, tool tilting angle and plunge depth as two main processing parameters are controlled by material flow and formation of dissimilar weld nugget. Also, high plunge depth of 0.4 mm possess a deteriorative influence on the joint strength due to excessive heating, inappropriate formation of macro- and micro-mechanical interlocks, formation of internal and surface defects, and high-volume fraction of big air bubbles. As can be found, the maximum ultimate tensile strength is around 45 MPa which attained at a tool tilting angle of 2° and a plunge depth of 0.2 mm. As shown in Fig. 15b–d, fracture location is varied by joint strength depending on the processing parameters. As seen in the cross section of tensile-failed samples, better intermixing and interlocking of dissimilar materials occurred at high heat inputs by increasing the tool tilting angle and plunge depth. Furthermore, it seems that the fracture is initiated by crack nucleation from the lower part at the retreating side between the SZ and U-antler and then propagated by separation of aluminum U-antler from the polymer part during changing of loading mode. Therefore, a tensile-shear fracture followed by the final tensile rupture can be proposed as the dominant mode. For the processed dissimilar joints in the tool tilting angles of 0° and 2°, the same trend can be observed, as shown in Fig. 15b, c. It can be caused by the strong bonding between aluminum at the TMAZ and polymer at SZ as well as

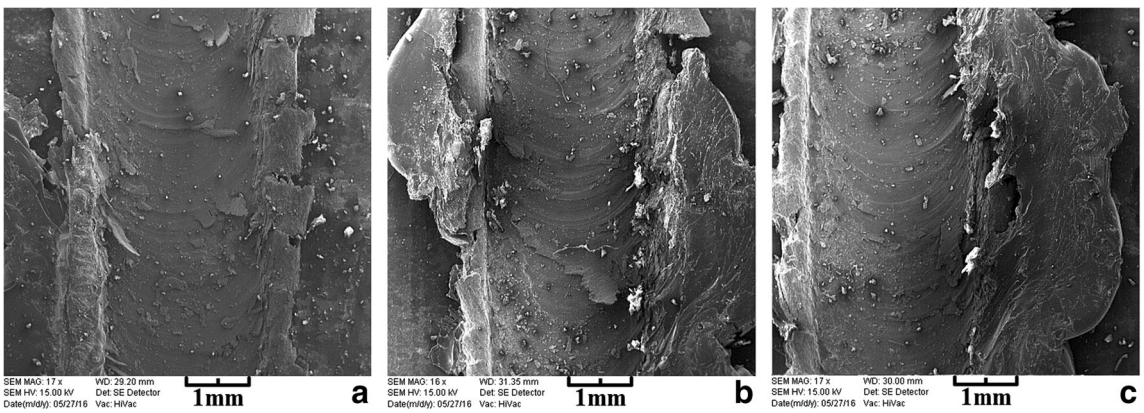

Fig. 16 Fracture surface appearances of the dissimilar FSWed joints with a tool tilt angle-plunge depth combination of 0°–0.1 mm (**a**), 2°–0.2 mm (**b**), and 2°–0.4 mm (**c**)

the high-interaction area due to larger aluminum U-antler. Some composite flashes with dark contrast from aluminum fragments within the polymer matrix are observable around the tensile samples which did not displayed noticeable influence on the fracture behavior. With increasing plunge depth up to 0.4 mm, fracture is mainly controlled by the detachment of polymer sheet from the mixed zone at the interface between the TMAZ of polymer and aluminum U-antler (see Fig. 15d). It seems that the higher tool penetration can reduce the strength of remained polymer ligament and it is the main reason for diminishing the mechanical strength at high plunge depth.

SEM images from the fracture surfaces of dissimilar FSWed joints at different tool tilting angles and plunge depths in the aluminum side are presented in Fig. 16. These fractographic features indicate that the existence of aluminum U-antler aids the strength of dissimilar joints. In addition, the presence of polymer materials within the aluminum micro-locks can approve the occurrence of chemical bonding during process. Furthermore, it can be easily found that the best geometry for macro- and micro-mechanical interlocks is formed at a processing condition including tool tilting angle of 2° and plunge depth of 0.2 mm. As expressed before in Fig. 15a, this processing parameter leads to the maximum tensile strength of dissimilar joint and can be considered as the optimum condition for dissimilar joining of AA5058 aluminum alloy and PMMA polymer by FSW process.

4 Conclusions

Dissimilar friction-stir lap joining of AA5058 aluminum alloy and PMMA polymer sheets was investigated. Influence of main processing parameters on the dissimilar welds formation, soundness, mechanical interlocking, interfacial chemical bonding, tensile properties, and fracture behavior was assessed. The main concluding remarks can be highlighted as follows:

- With increasing tool tilt angle in the range of 0–2°, the dissimilar materials intermixing was enhanced. While, the plunge depth variation in the range of 0.1–0.4 mm possess an optimum effect. Also, simultaneous increasing of tilt angle and decreasing of plunge depth leads to intensifying the air bubbles formation within the solidified polymer which can deteriorative the mixed zone soundness and property.
- Dissimilar bonding between the aluminum and polymer-based materials during FSW process was mainly due to mechanical interlocking by formation of an aluminum U-antler assisted by the chemical interfacial bonding. These mechanisms were affected by the processing parameters, significantly.
- Changing the tool tilting angle and plunge depth possess an impact influence on the shape and extension of U-antler macro-mechanical lock across the transverse section as well as the mixing morphology along the longitudinal section in transition from a flat to wavy interface.
- The processing parameters were optimized as tool tilt angle of 2° and plunge depth of 0.2 mm to form a dissimilar FSW with highest joint strength ratio of about 60%, with respect to the weakest polymer-based material.
- Fracture behavior of dissimilar joints was mainly controlled by the detachment of polymer material from the aluminum U-antler under the tensile-shear loading effect. Increasing the tilt angle and plunge depth by forming the bigger antlers with more mechanical interlocks can change the fracture mode and shift the failure location toward the polymer base side.

References

1. Bozkurt Y (2012) The optimization of friction stir welding process parameters to achieve maximum tensile strength in polyethylene sheets. Mater Des 35:440–445
2. Oliveira PHF, Amancio-Filho ST, dos Santos JF, Hage E Jr (2010) Preliminary study on the feasibility of friction spot welding in PMMA. Mater Lett 64:2098–2101
3. Amancio-Filho ST, Bueno C, dos Santos JF, Huber N, Hage E Jr (2011) On the feasibility of friction spot joining in magnesium/fiber-reinforced polymer composite hybrid structures. Mater Sci Eng A 528:3841–3848
4. Derazkola HA, Aval HJ, Elyasi M (2015) Analysis of process parameters effects on dissimilar friction stir welding of AA1100 and A441 AISI steel. Sci Technol Weld Join 20:553–562
5. Amancio-Filho ST, dos Santos JF (2009) Joining of polymers and polymer–metal hybrid structures: recent developments and trends. Polym Eng Sci 49:1461–1476
6. Bilici MK, Yükler Aİ, Kurtulmuş M (2011) The optimization of welding parameters for friction stir spot welding of high density polyethylene sheets. Mater Des 32:4074–4079
7. Matheny MP, Graff KF (2015) Ultrasonic welding of metals. In: Gallego-Juárez JA, Graff KF (eds) Power ultrasonics. Woodhead Publishing, Oxford, pp 259–293
8. Yan P, Güngör ÖE, Thibaux P, Liebeherr M, Bhadeshia HKDH (2011) Tackling the toughness of steel pipes produced by high frequency induction welding and heat-treatment. Mater Sci Eng A 528:8492–8499
9. Abibe AB, Amancio-Filho ST, dos Santos JF, Hage E Jr (2013) Mechanical and failure behaviour of hybrid polymer–metal staked joints. Mater Des 46:338–347
10. Blaga L, Bancilă R, dos Santos JF, Amancio-Filho ST (2013) Friction Riveting of glass–fibre-reinforced polyetherimide composite and titanium grade 2 hybrid joints. Mater Des 50:825–829
11. Balle F, Wagner G, Eifler D (2007) Ultrasonic spot welding of aluminum sheet/carbon fiber reinforced polymer – joints. Mater Werkst 38:934–938
12. Balle F, Wagner G, Eifler D (2009) Ultrasonic metal welding of aluminium sheets to carbon fibre reinforced thermoplastic composites. Adv Eng Mater 11:35–39

13. Balle F, Eifler D (2012) Statistical test planning for ultrasonic welding of dissimilar materials using the example of aluminum-carbon fiber reinforced polymers (CFRP) joints Statistische Versuchsplanung zum Ultraschallschweißen artfremder Werkstoffe am Beispiel von Aluminium-Kohlefaser-Kunststoff-Verbunden (CFK). Mater Werkst 43:286–292
14. Goushegir SM, dos Santos JF, Amancio-Filho ST (2014) Friction spot joining of aluminum AA2024/carbon-fiber reinforced poly(phenylene sulfide) composite single lap joints: microstructure and mechanical performance. Mater Des 54:196–206
15. Goushegir SM, dos Santos JF, Amancio-Filho ST (2015) Influence of process parameters on mechanical performance and bonding area of AA2024/carbon-fiber-reinforced poly(phenylene sulfide) friction spot single lap joints. Mater Des 83:431–442
16. Bergmann JP, Stambke M (2012) Potential of laser-manufactured polymer-metal hybrid joints. Phys Procedia 39:84–91
17. Mitschang P, Velthuis R, Didi M (2013) Induction spot welding of metal/CFRPC hybrid joints. Adv Eng Mater 15:804–813
18. Khodabakhshi F, Haghshenas M, Sahraeinejad S, Chen J, Shalchi B, Li J, Gerlich AP (2014) Microstructure-property characterization of a friction-stir welded joint between AA5059 aluminum alloy and high density polyethylene. Mater Charact 98:73–82
19. Eslami S, Ramos T, Tavares PJ, Moreira PMGP (2015) Effect of friction stir welding parameters with newly developed tool for lap joint of dissimilar polymers. Procedia Eng 114:199–207
20. Min J, Li Y, Li J, Carlson BE, Lin J (2014) Friction stir blind riveting of carbon fiber-reinforced polymer composite and aluminum alloy sheets. Int J Adv Manuf Technol 76:1403–1410
21. Shahmiri H, Movahedi M, Kokabi AH (2017) Friction stir lap joining of aluminium alloy to polypropylene sheets. Sci Technol Weld Join 22:120–126
22. Khodabakhshi F, Ghasemi Yazdabadi H, Kokabi AH, Simchi A (2013) Friction stir welding of a P/M Al–Al2O3 nanocomposite: microstructure and mechanical properties. Mater Sci Eng A 585:222–232
23. Mishra RS, Ma ZY (2005) Friction stir welding and processing. Mater Sci Eng R Rep 50:1–78
24. Khodabakhshi F, Simchi A, Kokabi A (2017) Surface modifications of an aluminum-magnesium alloy through reactive stir friction processing with titanium oxide nanoparticles for enhanced sliding wear resistance. Surf Coat Technol 309:114–123
25. Nandan R, DebRoy T, Bhadeshia HKDH (2008) Recent advances in friction-stir welding—process, weldment structure and properties. Prog Mater Sci 53:980–1023
26. Ma ZY (2008) Friction stir processing technology: a review. Metall Mater Trans A 39:642–658
27. Yusof F, Miyashita Y, Seo N, Mutoh Y, Moshwan R (2012) Utilising friction spot joining for dissimilar joint between aluminium alloy (A5052) and polyethylene terephthalate. Sci Technol Weld Join 17:544–549
28. Goushegir SM, dos Santos JF, Amancio-Filho ST (2014) Friction spot joining of aluminum AA2024/carbon-fiber reinforced poly(phenylene sulfide) composite single lap joints: microstructure and mechanical performance. Mater Des (1980-2015) 54:196–206
29. Khodabakhshi F, Haghshenas M, Chen J, Shalchi Amirkhiz B, Li J, Gerlich A (2017) Bonding mechanism and interface characterisation during dissimilar friction stir welding of an aluminium/polymer bi-material joint. Sci Technol Weld Join 22:182–190
30. Liu FC, Nakata K, Liao J, Hirota S, Fukui H (2014) Reducing bubbles in friction lap welded joint of magnesium alloy and polyamide. Sci Technol Weld Join 19:578–587
31. Ratanathavorn W, Melander A (2015) Dissimilar joining between aluminium alloy (AA 6111) and thermoplastics using friction stir welding. Sci Technol Weld Join 20:222–228
32. Derazkola HA, Khodabakhshi F, Simchi A (2017) Friction-stir lap-joining of aluminium-magnesium/poly-methyl-methacrylate hybrid structures: thermo-mechanical modelling and experimental feasibility study. Sci Technol Weld Join. https://doi.org/10.1080/13621718.2017.1323441
33. AK P, Raj R, Kailas SV (2015) A novel in-situ polymer derived nano ceramic MMC by friction stir processing. Mater Des 85:626–634
34. Simões F, Rodrigues DM (2014) Material flow and thermo-mechanical conditions during friction stir welding of polymers: literature review, experimental results and empirical analysis. Mater Des 59:344–351
35. Khodabakhshi F, Simchi A, Kokabi AH, Gerlich AP (2015) Friction stir processing of an aluminum-magnesium alloy with pre-placing elemental titanium powder: in-situ formation of an Al3Ti-reinforced nanocomposite and materials characterization. Mater Charact 108:102–114
36. Khodabakhshi F, Simchi A, Kokabi AH, Gerlich AP (2016) Similar and dissimilar friction-stir welding of an PM aluminum-matrix hybrid nanocomposite and commercial pure aluminum: microstructure and mechanical properties. Mater Sci Eng A 666:225–237
37. Khodabakhshi F, Simchi A, Kokabi A, Gerlich A, Nosko M, Švec P (2017) Influence of hard inclusions on microstructural characteristics and textural components during dissimilar friction-stir welding of an PM Al–Al2O3–SiC hybrid nanocomposite with AA1050 alloy. Sci Technol Weld Join 22:412–427
38. Mendes N, Neto P, Loureiro A, Moreira AP (2016) Machines and control systems for friction stir welding: a review. Mater Des 90: 256–265
39. Abibe AB, Sônego M, dos Santos JF, Canto LB, Amancio-Filho ST (2016) On the feasibility of a friction-based staking joining method for polymer–metal hybrid structures. Mater Des 92:632–642
40. Vigueras DJ, de Renero CT, Inal OT (2007) Explosive and impact welding: technical review. Mater Technol 22:200–204
41. Simar A, Bréchet Y, de Meester B, Denquin A, Gallais C, Pardoen T (2012) Integrated modeling of friction stir welding of 6xxx series Al alloys: process, microstructure and properties. Prog Mater Sci 57:95–183